Contrib Mineral Petrol (2007) 153:557–575
DOI 10.1007/s00410-006-0162-8

ORIGINAL PAPER

Cumulating processes at the crust-mantle transition zone inferred from Permian mafic-ultramafic xenoliths (Puy Beaunit, France)

Julien Berger · Olivier Féménias · Nicolas Coussaert · Jean-Claude C. Mercier · Daniel Demaiffe

Received: 3 December 2004 / Accepted: 25 October 2006 / Published online: 2 December 2006

Abstract Ultramafic and mafic xenoliths of magmatic origin, sampled in the Beaunit vent (northern French Massif Central), derive from the Permian (257 Ma) Beaunit layered complex (BLC) that was emplaced at the crust-mantle transition zone (~1 GPa). These plutonic xenoliths are linked to a single fractional crystallisation process in four steps: peridotitic cumulates; websteritic cumulates; Al-rich mafic cumulates (plagioclase, pyroxenes, garnet, amphibole and spinel) and finally low-Al mafic cumulates. This sequence of cumulates can be related to the compositional evolution of hydrous Mg basaltic magma that evolved to high-Al basalt and finally to andesitic basalt. Sr and Nd isotopic compositions confirm the co-genetic character of the various magmatic xenoliths and argue for an enriched upper mantle source comparable to present mantle wedges above subduction zones. LILE, LREE and Pb enrichment are a common feature of all xenoliths and argue for an enriched sub-alkaline transitional parental magma. The existence of a Permian magma chamber at 30 km depth suggests that the low-velocity zone observed locally beneath the Moho probably does not represent an anomalous mantle but rather a sequence of mafic/ultramafic cumulates with densities close to those of mantle rocks.

Keywords Xenoliths · Ultramafic-mafic · Sub-alkaline cumulate · Fractional crystallisation · Crust-mantle transition

Communicated by J. Hoefs.

J. Berger (✉)
Unité de Géologie Isotopique,
Musée Royal de l'Afrique Centrale,
3080 Tervuren, Belgium
e-mail: julien.berger@africamuseum.be

J. Berger · O. Féménias · D. Demaiffe
Laboratoire de Géochimie Isotopique et Géodynamique Chimique, DSTE, Université Libre de Bruxelles (CP 160/02),
50, av. Roosevelt, 1050 Bruxelles, Belgium

N. Coussaert
Unité de Minéralogie et Géochimie,
Musée Royal de l'Afrique Centrale,
3080 Tervuren, Belgium

J. Berger · J.-C. C. Mercier
CLDG, Université de La Rochelle, av. Crépeau,
17402 La Rochelle cedex 1, France

Introduction

The Puy Beaunit is a Cenozoic volcano from the Chaîne des Puys (French Massif Central) well known for its exceptional xenolith abundance and diversity (Brousse and Rudel 1964; Leyreloup 1974). Recent studies on mafic and ultramafic xenoliths have shown that they can be classified into two groups (Féménias et al. 2001, 2003): upper mantle xenoliths (lherzolites, harzburgites and dunites) and lower crustal mafic and ultramafic magmatic xenoliths derived from a deep-seated layered intrusion ''Beaunit layered complex (BLC)'': peridotites, websterites, plagioclase and garnet pyroxenites, garnet- and amphibole-bearing gabbronorites and composite mafic/ultramafic xenoliths. The ultramafic magmatic xenoliths have strong calc-alkaline characters (enrichment in LILE, depletion in Nb, Ta, Zr and Hf; Féménias et al. 2003) but the mafic magmatic samples (as will be demonstrated in this paper) do not show typical calc-alkaline or tholeiitic

whole-rock geochemical features. However, the various lithologies and mineral compositions are comparable to what is observed in roots of calc-alkaline island arcs (Berger et al. 2005).

The discrimination between calc-alkaline and tholeiitic affinity of mafic magmatic rocks is well established for lavas but still poorly constrained for basic plutonic xenoliths because fractional crystallisation processes (cumulation) partly erase the information about magma composition. The main geochemical differences between calc-alkaline and tholeiitic lavas are (Miyashiro 1974; Grove and Baker 1984; Sisson and Grove 1993; Müntener et al. 2001; Grove et al. 2003): a high H_2O content, a strong SiO_2 enrichment with constant FeO/MgO ratio and a pronounced LILE enrichment with negative Nb and Ta anomalies for calc-alkaline lavas, whereas the tholeiitic series show iron enrichment during differentiation with nearly constant SiO_2 content but a strong depletion in the most incompatible elements (LILE and LREE). Calc-alkaline lava and plutonic series are also characterised by the relatively high abundance of amphibole and sometimes of magmatic garnet; these phases are present in minor proportions or absent in tholeiitic series (Green and Ringwood 1968; Cawthorn and O'Hara 1976; Foden and Green 1992; Harangi et al. 2001). Calc-alkaline deep intrusions are generally characterised by a high proportion of pyroxenites but a rather low proportion of plagioclase (late crystallising phase in H_2O-poor magmas and absent in H_2O-rich magmas; Müntener et al. 2001). In tholeiitic plutons plagioclase is abundant, it is an early crystallising phase at low-*P* but a late crystallising phase at high-*P* (Villiger et al. 2004), while amphibole is a minor phase and garnet is generally absent. Moreover, plagioclase is highly calcic in the hydrous calc-alkaline series (Sisson and Grove 1993) due to high H_2O content of the melt.

Lower crustal xenoliths are samples of the in situ crust-mantle transition zone in continental areas. In general, they suffered only minor exhumation-related retrogression compared to outcropping massifs of deep-seated origin. The lower crust is generally composed of mafic rocks (Griffin and O'Reilly 1987; Downes 1993; Rudnick and Fountain 1995) although in Variscan Western Europe, abundant felsic and metasedimentary rocks are thought to co-exist with the mafic granulites (Leyreloup 1974; Villaseca et al. 1999). Such mafic deep-seated rocks can be divided into two main groups: (1) granulites considered as high-pressure crystallisation (1 GPa) products of underplated basaltic magmas coeval with HT granulitic metamorphism in a late orogenic setting (Downes et al. 1990; Upton et al. 2001) and (2) high pressure mafic/ultramafic magmatic rocks with no granulite facies overprint (Singh and McKenzie 1993). Underplating of basic magmas plays a major role in the evolution of the lowermost crust. This process can account for the complex structure of the crust-mantle boundary; indeed mafic intrusions can be interlayered with mafic, felsic or metasedimentary granulites and even with uppermost mantle (Griffin and O'Reilly 1987; Chen et al. 2001). Consequently, the petrological crust-mantle boundary (mantle rocks topped by magmatic or metamorphic rocks) can differ from the geophysical Moho (abrupt change in *P*-wave velocity) because mafic/ultramafic lower crustal rocks can be denser than the underlying mantle (Jull and Kelemen 2001; Müntener et al. 2001).

The xenolithic nature of the Beaunit layered rocks precludes a general structural and stratigraphic investigation of the magmatic xenoliths. Nevertheless, the large size of some xenoliths (up to 10 cm) allows a detailed study of the main lithologies. We present petrological and geochemical data for representative magmatic samples of the main rock-types (major and trace elements; Sr–Nd isotopic data) and for rock-forming minerals (trace elements by LA-ICP-MS). The aims of this paper are to clarify the geochemical relationship between magmatic ultramafic and mafic samples, to discriminate the calc-alkaline or tholeiitic affinity of the mafic samples and to shed some light on magma differentiation processes in the crust-mantle transition zone. Compilation of the data published on upper mantle and lower crustal xenoliths from Beaunit will also be done in order to constrain the crust-mantle boundary structure beneath northern French Massif Central.

Geological setting and summary of previous works

Puy Beaunit is a Quaternary maar (Baudry and Camus 1970; Camus 1975), dated at 43900 ± 5100 a (Rosseel 1996) and situated at the northernmost end of the Chaîne des Puys in the French Massif Central (Fig. 1). The magmatic mafic/ultramafic xenoliths come from the BLC that was emplaced at 257 ± 6 Ma (U–Pb SIMS dating on a 1.5 mm zircon crystal recording a magmatic or late magmatic sub-solidus equilibration age (Féménias et al. 2003). They belong to the ''semelle gabbro-norite-peridotite'' of Leyreloup (1974), i.e. cumulates with little or no granulitic facies metamorphic overprint. Acid meta-igneous xenoliths are generally associated with these mafic xenoliths by an AFC process (Downes et al. 1990). Unfortunately, at Beaunit, the felsic xenoliths have always partially melted in

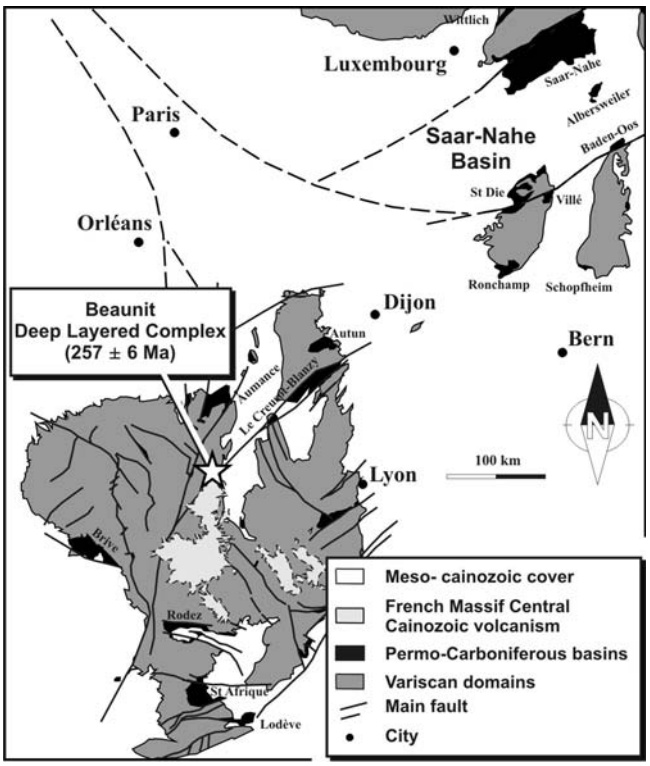

Fig. 1 Geological sketch showing the location of Puy Beaunit and Permo-Carboniferous basins in NW Europe

response to transport in the host lava and they have been largely contaminated by the host basalt (Brousse and Rudel 1964); they were thus not integrated in the study. The BLC belongs to the large Permo-Carboniferous within-plate magmatic province (often with calc-alkaline geochemical signature) observed across Europe and North Africa (see references in Féménias et al. 2003, Fig. 1). It corresponds to a mafic underplating event spatially controlled by post-Variscan trans-tensional to trans-pressional basin tectonics in an intracontinental setting. The main fault responsible for the onset of Permian magmatism at Beaunit is the lithospheric Blanzy-Le Creusot fault, located in the vicinity of the Puy Beaunit vent (Féménias et al. 2003).

The magmatic mafic xenoliths crystallised in a narrow T range, close to 1000°C, at a mean pressure of 1 GPa. They have undergone a sub-solidus recrystallisation, at 700–800°C and 1 GPa. This event is interpreted as the late-magmatic isobaric cooling (Berger et al. 2005). During ascent of the xenoliths to the surface in the Quaternary lava, some mafic rocks have undergone a HT-LP metamorphic overprinting that was responsible for destabilisation of some primary magmatic phases. Garnet is destabilised into plagioclase-orthopyroxene-spinel symplectites. Amphibole is transformed to clinopyroxene-plagioclase-spinel symplectites. Locally, at the contact with the host lava, primary orthopyroxene and clinopyroxene were partially melted (Faure et al. 2001; Berger et al. 2005).

Mantle xenoliths from Beaunit are compositionally varied, ranging from relatively fertile spinel lherzolites to refractory spinel dunites. Fertile peridotites have registered a modal (amphibole-bearing lherzolites) and cryptic metasomatic event that took place before the last Permian (257 Ma) melting episode. Depletion processes are related to two major melt extraction episodes (Féménias et al. 2004). The first melting event and metasomatic enrichment are attributed to an ancient fluid infiltration that could be related to a pre-Variscan regional subduction (located to the north of the Beaunit area). Texture acquisition and major deformation of the mantle xenoliths were sub-contemporaneous with the subduction and would have resulted from lithospheric delamination. The second melting event produced high-Mg basalts with calc-alkaline trace element signatures that gave rise to the Permo-carboniferous underplating episode (BLC emplacement). The subduction-related geochemical signature of the ultramafic magmatic suite has thus been interpreted as resulting from the passive remobilisation of a mantle source, which was previously metasomatised during Variscan subduction.

Analytical methods and sample selection

Xenoliths were selected for whole-rock geochemical analysis on the basis of two criteria: their size (mini-

mum material required for representative analysis) and minor contamination (<1%) of the xenolith by the host lava. Trace elements in clinopyroxene and plagioclase were analysed by in situ Laser Ablation ICP-MS (Table 1). The data were collected with a UV Fison laser probe coupled to a VG elemental Plasmaquad (PQ2 Turbo Plus) ICP-MS (Musée Royal de l'Afrique Centrale at Tervuren). Each analysis is a mean of 3–7 spots. The standard deviation (2σ) is comprised between 2 and 20% for the REE, Zr and Hf in clinopyroxene and LREE, Ba and Sr in plagioclase. For the trace elements with concentration <1 ppm (Nb, Rb in both minerals; HREE, Zr and Hf in plagioclase; Ba and Sr in clinopyroxene) it is generally between 20 and 200%. Analytical methods, detection limits, precision and accuracy are detailed in Féménias et al. (2003).

Whole-rock major and transition elements composition (Table 2) has been obtained by X-ray fluorescence spectrometry at the "Collectif inter-institutionnel de géochimie instrumentale" (University of Liège). The description of the method can be found in Bologne and Duchesne (1991) and Féménias et al. (2003). REE and other trace element concentrations have been measured by ICP-MS (Table 2), also at the University of Liège (detailed procedure can be found in Vander Auwera et al. (1998) and Féménias et al. (2003). Whole-rock major and trace-element compositions of ultramafic samples come from Féménias et al. (2003). Measurements of Sr and Nd isotopic ratios (Table 3) were carried at the GIGC (University of Brussels) on a VG Sector 54 multicollector thermal ionisation mass spectrometer. Analytical method and instrumental techniques are detailed in Ashwal et al. (2002).

Petrography

The magmatic ultramafic to mafic plutonic xenoliths from Beaunit are either homogeneous or finely layered. Major rock types are peridotites, pyroxenites and gabbros; composite mafic/ultramafic xenoliths are common. All ultramafic rocks are devoid of plagioclase and contain spinel (less than 2%); they have been described previously by Féménias et al. (2003). They have been sub-divided in two main groups: (1) peridotites (lherzolite, harzburgite and dunite) and (2) websterites (ol-, cpx-, and opx-websterites).

The mafic xenoliths are plagioclase bearing but olivine-absent rocks. They are either homogeneous monolithologic rocks or well-layered rocks. The layered samples show asymmetric anorthositic and pyroxenitic layers (see Fig. 4 in Féménias et al. 2001)

Table 1 Trace elements contents (ppm) obtained by LA-ICP-MS for plagioclase and clinopyroxene of magmatic xenoliths from Puy Beaunit

Sample	PBN 98-60	PBN 98-63	PBN 98-73	PBN 98-80	PBN 98-86	PBN 98-87	PBN 98-88	PBN 98-92	Mean 2σ(%)	PBN 86-19	PBN 98-60	PBN 98-63	PBN 98-73	PBN 98-80	PBN 98-83	PBN 98-86	PBN 98-87	PBN 98-88	PBN 98-92	Mean 2σ(%)
Mineral	Plag	Plag	Plag	Plag	Plag	Plag	Plag	Plag		Cpx	Cpx	Cpx	Cpx	Cpx	Cpx	Cpx	Cpx	Cpx	Cpx	
Rb	0.2	0.2	0.6	0.1	1.0	0.6	0.4	0.4	82	<DL	<DL	0.3	<DL	<DL	<DL	<DL	0.2	<DL	<DL	230
Sr	751	354	748	750	307	392	1085	421	14	56	26	18	25	35	56	10	15	57	52	25
Ba	20	36	19	27	142	123	1318	68	20	2.9	0.9	6.0	2.4	2.1	2.1	0.7	2.4	76.0	10.4	61
Zr	0.2	<DL	1.6	0.3	0.5	0.2	11.7	<DL	134	12	6	69	27	153	96	318	85	139	96	11
Hf	<DL	<DL	<DL	<DL	0.1	<DL	0.3	<DL	151	0.4	0.2	1.7	1.0	5.2	3.4	9.4	1.9	4.3	3.4	9
Nb	<DL	<DL	<DL	<DL	<DL	<DL	0.3	0.3	70	0.2	0.2	0.6	0.5	0.2	0.3	0.3	<DL	1.2	1.4	98
La	0.3	1.8	1.6	4.1	7.0	2.3	4.7	8.4	6	2.5	0.8	2.6	1.3	3.9	2.4	5.4	2.2	6.3	6.5	20
Ce	0.7	3.0	3.2	6.7	10.0	3.8	9.6	15.4	15	12.8	3.0	11.6	6.2	18.9	8.7	20.0	8.1	19.6	30.8	27
Nd	0.5	1.0	1.5	2.4	3.1	1.3	3.8	4.8	28	14.6	5.1	14.5	9.6	25.5	11.2	26.1	9.8	18.7	39.4	29
Sm	0.1	0.1	0.4	0.3	0.6	0.2	0.6	0.5	31	3.5	1.5	4.4	2.8	7.6	4.0	10.0	2.8	4.3	11.7	16
Eu	0.3	0.2	0.4	1.1	1.1	0.4	0.6	1.1	29	0.7	0.7	0.9	1.0	1.9	1.0	1.8	0.9	0.8	1.9	18
Gd	0.14	<DL	0.4	0.4	0.6	0.2	0.5	0.5	33	2.5	0.8	4.4	2.2	7.8	5.7	16.2	4.1	3.9	14.7	11
Dy	<DL	<DL	0.3	0.3	0.4	0.1	0.3	0.3	87	1.5	0.4	4.5	1.4	6.3	5.9	23.9	4.3	3.1	14.2	23
Er	0.1	<DL	0.1	0.2	0.3	0.1	0.2	0.1	74	0.6	0.1	2.4	0.4	2.6	1.7	15.4	2.5	1.5	5.9	31
Yb	0.12	<DL	0.1	0.2	0.3	0.1	0.2	0.1	98	0.6	0.1	2.3	0.1	1.6	0.6	12.7	1.9	1.3	4.8	24
An	94	77	91	62	61	66	92	70		89	82	78	83	76	81	74	81	84	86	
$Mg^{\#}$																				

<DL below semi-quantitative detection limits

Table 2 Bulk-rock analyses of representative mafic xenoliths from Beaunit

Sample	PBN 98-60 Grt-gbn	PBN 98-62 Amp-gbn	PBN 98-63 Amp-gbn	PBN 98-73 Grt-gbn	PBN 98-75 Grt-gbn	PBN 98-76 Pol-gbn	PBN 98-77 Grt-gbn	PBN 98-79 Grt-gbn	PBN 98-80 Amp-gbn	PBN 98-82 Pol-gbn	PBN 98-83 Grt-cpxite	PBN 98-86 Pol-gbn	PBN 98-87 Pol-gbn	PBN 98-88 Cpxite	PBN 98-92 Pol-gbn	PBN 98-101 Norite	PBN 98-103 Amp-gbn	PBN 98-106 Pol-gbn	PBN 98-114 Pol-gbn
Major elements (wt%)																			
SiO_2	42.50	46.70	45.89	43.31	39.46	43.41	43.96	43.07	42.95	50.15	41.22	48.37	50.39	46.58	49.85	48.92	50.72	50.86	50.21
TiO_2	0.60	0.53	0.87	0.60	2.35	0.65	0.53	0.38	0.87	0.44	0.72	1.31	0.31	0.79	0.62	1.13	0.46	1.09	0.41
Al_2O_3	18.46	20.65	17.94	18.77	25.53	17.69	15.89	17.23	20.51	17.16	16.62	16.48	17.80	15.73	17.62	14.73	17.27	19.43	12.28
Fe_2O_3	13.62	9.27	10.57	13.17	15.42	16.68	10.86	12.79	13.89	7.35	16.26	11.52	7.97	8.29	8.34	13.44	7.49	10.53	12.36
MnO	0.21	0.15	0.16	0.24	0.43	0.30	0.16	0.20	0.19	0.13	0.44	0.18	0.14	0.15	0.14	0.20	0.13	0.17	0.21
MgO	9.52	7.71	7.75	8.76	7.05	7.32	10.97	10.94	6.24	10.30	11.17	8.71	9.22	8.58	9.29	13.74	9.84	5.25	15.55
CaO	13.67	12.42	14.94	13.62	8.75	13.00	16.98	14.12	13.71	12.29	12.55	10.84	11.25	19.06	11.45	6.81	11.64	8.79	7.94
Na_2O	0.33	1.89	1.72	0.74	0.83	1.37	1.00	0.60	1.13	2.01	0.89	2.59	2.22	1.01	2.27	0.82	2.42	2.78	1.02
K_2O	0.05	0.19	0.22	0.11	0.14	0.11	0.03	0.06	0.08	0.18	0.14	0.40	0.19	0.10	0.32	0.12	0.35	0.74	0.12
P_2O_5	0.02	0.06	0.06	0.04	0.05	0.05	0.01	0.01	0.03	0.05	0.04	0.13	0.02	0.06	0.08	0.04	0.06	0.32	0.03
Sum	98.97	99.58	100.12	99.36	100.01	100.58	100.40	99.40	99.59	100.04	100.04	100.54	99.51	100.35	99.98	99.95	100.39	99.95	100.13
$Mg^{\#}$	55.47	59.71	56.67	54.26	44.90	43.90	64.30	60.39	44.46	71.42	55.04	57.39	67.34	64.87	66.52	64.58	70.09	47.04	69.16
Trace elements (ppm)																			
Cr	267	116	166	88	655	16	249	159	66	467	217	323	412	77	1097	594	510	29	962
Ni	32	41	42	35	62	17	46	70	36	158	27	95	129	40	25	135	100	27	228
Co	48	47	44	40	41	45	43	48	32	40	41	44	49	29	36	50	40	35	58
Rb	0.85	3.33	2.81	1.25	1.99	0.26	0.09	0.59	0.67	2.08	1.92	5.94	0.85	0.88	3.76	0.65	6.19	3.50	1.27
Cs	0.03	0.10	0.09	0.06	0.07	0.01	0.13	0.14	0.12	0.13	0.12	0.16	0.04	0.07	0.08	0.04	0.11	0.07	0.03
Sr	166	562	317	196	293	294	146	125	378	152	143	180	208	357	318	152	152	716	84
Ba	13	93	110	37	111	35	6	29	63	51	52	130	62	130	134	83	61	480	30
Zr	7.6	21.0	39.6	12.6	87.3	12.1	0.2	0.1	1.0	28.5	50.7	89.2	8.9	94.4	48.1	45.88	22.46	84.20	6.96
Hf	0.19	0.55	1.42	0.22	2.59	0.25	0.20	0.21	0.21	0.95	1.88	2.74	0.31	3.25	1.37	1.64	0.61	2.69	0.22
Nb	1.06	5.65	5.21	2.60	68.64	2.72	0.71	1.13	1.96	3.74	4.10	9.55	2.00	3.28	7.33	2.63	4.84	8.41	2.65
Ta	0.07	0.37	0.33	0.22	6.03	0.20	0.17	0.17	0.17	0.29	0.33	0.70	0.17	0.34	0.51	0.19	0.39	0.45	0.19
U	0.05	0.12	0.09	0.04	0.16	0.01	0.07	0.10	0.11	0.10	0.10	0.25	0.02	0.28	0.18	0.17	0.26	0.12	0.04
Th	0.25	0.85	0.46	0.30	0.27	0.07	0.01	0.01	0.05	0.38	0.35	1.04	0.14	1.46	1.08	0.73	0.98	0.45	0.17
Y	5.39	5.69	20.58	9.10	100.30	11.01	4.00	4.19	7.69	11.01	32.57	46.00	7.37	21.78	16.82	28.37	9.48	26.21	4.89
Pb	0.85	1.37	1.17	2.15	1.33	0.98	0.80	0.58	2.11	0.63	2.46	2.18	1.23	0.85	1.98	1.21	1.07	6.53	2.56
La	1.57	7.77	7.25	3.09	6.97	3.54	0.48	1.28	3.05	4.61	4.71	12.38	3.86	10.36	12.28	8.42	6.41	23.41	2.58
Ce	2.67	12.50	16.25	7.43	9.26	8.61	1.70	2.90	6.87	9.93	11.55	26.48	7.91	31.72	26.96	19.06	12.28	51.49	5.05
Pr	0.39	1.42	2.32	0.94	0.92	1.17	0.31	0.47	0.86	1.21	1.54	3.08	0.96	5.01	3.77	2.48	1.45	6.74	0.59
Nd	2.07	4.95	10.64	3.93	3.65	5.31	1.62	2.26	4.34	5.39	6.79	13.52	4.01	24.17	16.15	10.99	4.93	28.38	2.18
Sm	0.64	1.15	3.09	1.00	1.99	1.48	0.52	0.66	1.13	1.48	2.13	3.86	0.88	6.07	4.01	2.84	1.14	6.54	0.51
Eu	0.40	0.60	0.81	0.58	0.82	0.62	0.49	0.42	0.71	0.65	0.74	1.21	0.52	1.38	1.09	0.87	0.55	2.07	0.28
Gd	0.86	1.18	3.21	0.97	6.31	1.54	0.68	0.72	1.31	1.64	3.33	5.17	0.82	4.87	3.29	3.64	1.18	5.95	0.58
Tb	0.15	0.18	0.51	0.18	1.52	0.28	0.14	0.12	0.24	0.31	0.70	0.91	0.14	0.68	0.49	0.67	0.24	0.81	0.11
Dy	0.99	1.14	3.50	1.38	12.97	1.90	0.85	0.84	1.49	1.92	4.87	6.91	1.03	4.04	2.89	4.56	1.39	4.75	0.82
Ho	0.22	0.22	0.71	0.32	3.69	0.44	0.18	0.18	0.32	0.44	1.15	1.72	0.24	0.77	0.58	1.03	0.32	0.97	0.19
Er	0.63	0.66	2.22	1.00	11.54	1.24	0.51	0.50	0.95	1.31	2.98	4.75	0.73	2.15	1.68	2.99	0.96	2.55	0.59
Tm	0.09	0.09	0.35	0.17	1.84	0.21	0.13	0.08	0.16	0.21	0.40	0.66	0.12	0.32	0.24	0.46	0.14	0.39	0.09
Yb	0.60	0.62	2.22	1.07	12.69	1.37	0.46	0.47	0.89	1.24	2.39	4.36	0.72	1.80	1.54	2.92	0.95	2.43	0.56
Lu	0.07	0.08	0.31	0.15	2.01	0.21	0.09	0.08	0.12	0.17	0.30	0.64	0.09	0.25	0.18	0.39	0.14	0.36	0.08

Amp-gbn amphibole-gabbronorite, *pol-gbn* polygonal-gabbronorite, *grt-gbn* garnet-gabbronorite, *grt-cpxite* garnet-clinopyroxenite, *cpxite* clinopyroxenite

Table 3 Sr–Nd isotopic data of mantle and magmatic xenoliths from Puy Beaunit

	Rb	Sr	$^{87}Sr/^{86}Sr$	2 σ	$(^{87}Sr/^{86}Sr)_i$	Sm	Nd	$^{143}Nd/^{144}Nd$	2 σ	$(^{143}Nd/^{144}Nd)_i$	$(\varepsilon_{Nd})_i$
Mantle xenoliths											
PBN 98-07	2.91	32.22	0.706281	0.000010	0.705319	0.58	3.83	0.512338	0.000008	0.512185	–2.4
PBN 98-08	2.98	31.10	0.704344	0.000008	0.703331	0.60	2.61	0.512818	0.000018	0.512584	5.4
PBN 98-14	2.60	40.12	0.706890	0.000005	0.706202	0.77	4.63	0.512325	0.000008	0.512156	–3.0
PBN 98-19	2.10	16.40	0.706338	0.000006	0.704984	0.44	2.69	0.512344	0.000015	0.512178	–2.5
PBN 98-51	0.54	9.81	0.704459	0.000011	0.703876	0.08	0.39	–	–	–	–
PBN 98-53	5.50	50.10	0.704335	0.000006	0.703174	0.50	3.02	0.512598	0.000016	0.512430	2.4
PBN 98-74	0.75	20.99	0.705243	0.000008	0.704865	0.11	0.68	–	–	–	–
PBN 98-90	0.86	18.00	0.704161	0.000010	0.703659	0.10	0.49	0.51259	0.000043	0.512392	1.7
Beaunit layered complex											
Ultramafic											
PBN 86-19	2.09	16.40	0.704784	0.000008	0.703436	0.44	2.69	0.512361	0.000008	0.512194	–2.2
PBN 86-24	5.00	53.51	0.704432	0.000007	0.703444	0.80	4.07	0.512734	0.000007	0.512534	4.4
PBN 98-01	1.57	50.40	0.703914	0.000008	0.703585	0.05	0.20	0.512669	0.000007	0.512423	2.3
PBN 98-05	1.51	37.49	0.704291	0.000010	0.703865	0.77	3.82	0.512185	0.000010	0.511980	–6.4
PBN 98-09	1.24	15.93	0.704896	0.000008	0.704073	0.34	1.31	0.512867	0.000015	0.512604	5.8
PBN 98-13	1.40	8.85	0.705415	0.000008	0.703742	0.15	1.01	0.512296	0.000027	0.512142	–3.2
PBN 98-39	4.04	37.80	0.703860	0.000010	0.702730	0.97	3.80	0.512643	0.000013	0.512385	1.5
Mafic											
PBN 98-60	0.85	166.50	0.705139	0.000009	0.705085	0.64	2.07	–	–	–	–
PBN 98-62	3.33	561.84	0.703589	0.000005	0.703526	1.15	4.95	0.512776	0.000009	0.512540	4.6
PBN 98-63	2.81	316.86	0.704427	0.000005	0.704333	3.09	10.64	0.512653	0.000011	0.512357	1.0
PBN 98-73	1.25	195.96	0.704988	0.000006	0.704921	1.00	3.93	0.512631	0.000010	0.512371	1.3
PBN 98-75	1.99	292.84	0.705906	0.000006	0.705834	1.99	3.65	0.512905	0.000011	0.512351	0.8
PBN 98-76	0.26	293.57	0.704821	0.000007	0.704812	1.48	5.31	0.512338	0.000008	0.512055	–4.9
PBN 98-77	0.09	145.68	0.703556	0.000006	0.703550	0.52	1.62	0.512955	0.000010	0.512625	6.2
PBN 98-79	0.59	125.27	0.705080	0.000006	0.705030	0.66	2.26	–	–	–	–
PBN 98-80	0.67	377.96	0.704145	0.000007	0.704126	1.13	4.34	0.512621	0.000006	0.512357	1.0
PBN 98-82	2.08	152.49	0.704167	0.000006	0.704023	1.48	5.39	0.512751	0.000008	0.512473	3.2
PBN 98-83	1.93	142.96	0.704575	0.000006	0.704433	2.13	6.79	0.512616	0.000013	0.512297	–0.2
PBN 98-86	5.94	180.06	0.705196	0.000005	0.704847	3.86	13.52	0.512701	0.000010	0.512411	2.0
PBN 98-87	0.85	207.51	0.706262	0.000005	0.706219	0.88	4.01	0.512519	0.000010	0.512295	–0.2
PBN 98-88	0.90	357.10	0.705902	0.000007	0.705875	6.07	24.17	0.512321	0.000009	0.512066	–4.7
PBN 98-92	3.76	318.43	0.705544	0.000005	0.705419	4.01	16.15	0.512387	0.000009	0.512134	–3.4
PBN 98-101	0.65	151.96	0.704562	0.000005	0.704517	2.84	10.99	0.512490	0.000012	0.512228	–1.6
PBN 98-103	6.19	151.55	0.704110	0.000005	0.703678	1.14	4.93	0.512711	0.000008	0.512476	3.3
PBN 98-106	3.50	716.46	0.705517	0.000005	0.705465	6.54	28.38	0.512536	0.000010	0.512302	–0.1
PBN 98-114	1.27	83.91	0.705214	0.000005	0.705054	0.51	2.18	–	–	–	–

similar to those observed in typical stratiform intrusions such as the Bushveld and the Skaergaard complexes (Cawthorn 1996). These layers are outlined by sharp contacts marked by the appearance or disappearance of a phase (phase layering) but, in a given layer, the modal proportions of cumulus phases vary gradually (modal layering). The lithologies vary from leuco-gabbronorites (plagioclase-rich) to mela-gabbronorites (pyroxenes-rich) with minor gabbros, norites and plagioclase-bearing pyroxenites. All the plagioclase-bearing rocks show equigranular and polygonal textures. These textures and the lack of apparent zoning between core and rim of the silicate phases are typical features of late-magmatic sub-solidus recrystallised assemblages during the slow cooling of the deep-seated intrusion (Berger et al. 2005). The main rock-forming minerals are plagioclase, orthopyroxene, clinopyroxene, garnet and amphibole (a table with the modal proportions of mafic samples can be found in Berger et al. 2005). No exsolutions were observed in pyroxenes. The garnet is always transformed into a fine-grained plagioclase-orthopyroxene-spinel symplectite (Berger et al. 2005). Common accessory minerals are spinel and ilmenite. Other accessory phases (Ti-rich phlogopite, rutile, armacolite, pyrrhotite, pentlandite, zircon and srilankite) are very scarce, they have been observed in one Zr-rich micro-layer of a composite xenolith (Féménias et al. 2005). Apatite has only been observed as inclusions into antiperthitic plagioclase from gabbronorite PBN 98-106.

The selected mafic xenoliths studied in this paper have been subdivided into:

(1) euhedral garnet-bearing rocks (Fig. 2a): the primary habit of the retrogressed garnet (transformed into orthopyroxene-plagioclase-spinel symplectites) is subhedral to euhedral; it was in textural equilibrium with plagioclase and/or clinopyroxene. This group includes a garnet-plagioclase-pyroxenite (PBN 98-83) and an ilmenite-rich (~8 vol%) garnet-anorthosite (PBN 98-75). These rocks have been interpreted as garnet cumulates (Berger et al. 2005);
(2) interstitial garnet-bearing rocks (Fig. 2b): the retrogressed garnet is anhedral and located at the contacts between the main silicates. It probably results from the reaction of plagioclase and pyroxenes during cooling of the intrusion (Berger et al. 2005). This group is composed of layered gabbros and gabbronorites;
(3) gabbronorites with polygonal texture (Fig. 2c): they are plagioclase-orthopyroxene-clinopyroxene-spinel rocks with no garnet and amphibole. PBN 98-92 and PBN 98-106 are very fine-grained compared to the others. PBN 98-106 also contains apatite (less than 1%);
(4) amphibole gabbronorites (Fig. 2d): these gabbronorites contain preserved (relics) and/or more or less largely retrogressed (into clinopyroxene-plagioclase-titanomagnetite symplectites) subhedral to euhedral brown amphibole (Ti-pargasite);
(5) a norite s.s. (PBN 98-101): it is finely layered and composed only by plagioclase and orthopyroxene;
(6) a plagioclase clinopyroxenite (PBN 98-88): it is characterized by the simple association of clinopyroxene and plagioclase.

Mineral chemistry

Major elements variation

The main characteristics of the major element mineral chemistry of the magmatic ultramafic and mafic samples have already been discussed in recent publications (Féménias et al. 2001, 2003; Berger et al. 2005). They are only briefly summarised in here. Olivine is only present in ultramafic samples; its composition varies from Fo_{90-83} in the peridotites to Fo_{85-78} in the websterites. Clinopyroxene is a diopside in the ultramafic samples and a diopside-augite in the gabbros ($Mg^{\#}$: 92.5–81.5 and 88–65, respectively). The Al content increases with decreasing $Mg^{\#}$ for clinopyroxene with $Mg^{\#} > 76$: from 0.06 to 0.16 a.p.f.u. for ultramafic samples and from 0.15 to 0.35 in the mafic rocks (Fig. 3). But, for clinopyroxenes with $Mg^{\#}<76$, the Al content decreases (from 0.35 to 0.08 a.p.f.u.). The orthopyroxene $Mg^{\#}$ ranges from 90 to 84 in the peridotites, from 85 to 79 in the websterites and from 80 to 52 in the mafic sequence. Plagioclase is highly calcic (An_{94-82}) in the garnet-bearing mafic samples, slightly less An-rich (An_{87-62}) in the amphibole gabbronorites and intermediate (An_{72-48}) in the polygonal gabbron-

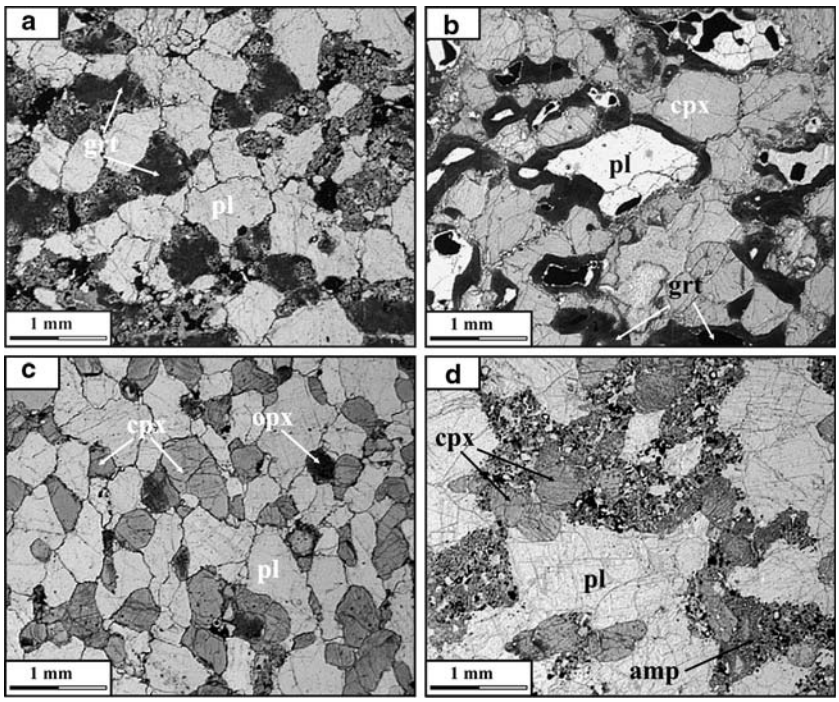

Fig. 2 Microphotographs of mafic xenoliths (plane-polarised light) illustrating the various cumulate groups. **a** Ilmenite-rich (~8 vol%) garnet-anorthosite PBN 98-75: the primary habitus of the retrogressed garnet is subhedral to euhedral; it is in textural equilibrium with plagioclase and/or clinopyroxene. **b** Garnet-bearing gabbro PBN 98-60: the retrogressed anhedral garnet is located at the contacts between the main silicates. **c** Gabbronorite PBN 98-87 with polygonal texture. **d** Amphibole gabbronorite PBN 98-63 showing partly preserved and more or less retrogressed subhedral to euhedral brown amphibole (Ti-pargasite)

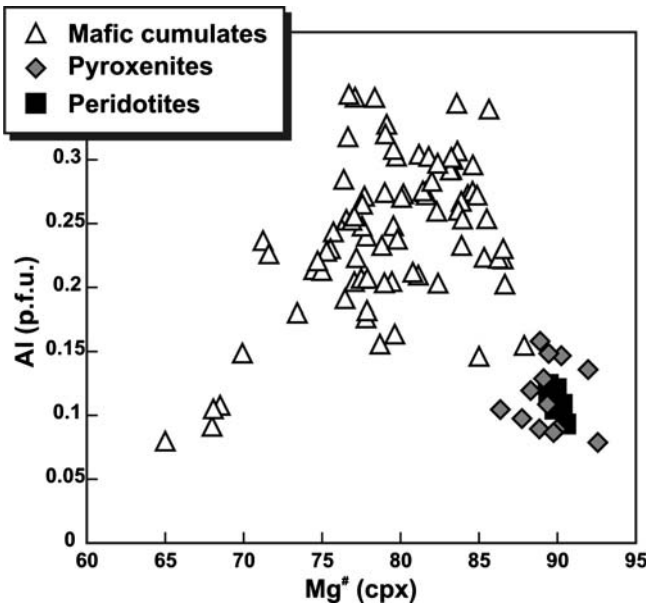

Fig. 3 Co-variation of Mg# and Al content in clinopyroxenes from BLC, data from Féménias et al. (2003) and Berger et al. (2005)

orites. Garnet is almandine-pyrope rich, with a significant grossular content and a low spessartine content ($Alm_{42\text{-}45}Grs_{9\text{-}21}Prp_{35\text{-}47}Sps_{1\text{-}2}$).

Trace elements contents

In situ laser ablation ICP-MS trace elements (REE, Ba, Nb, Sr, Zr and Hf) analyses of plagioclase and clinopyroxene (Fig. 4) have been obtained on the mafic samples and on an opx-websterite (PBN 86-19). Plagioclase shows well-defined LREE enrichment ($(La/Yb)_N$: 2–50) and a strong positive Eu anomaly (Eu/Eu^*: 3–9). Clinopyroxene generally displays a convex upward REE pattern with a slight negative Eu anomaly (Fig. 4). Clinopyroxene from garnet-bearing samples (PBN 98-60, 98-73, 98-83) is significantly depleted in HREE compared to the other samples. This is classically observed for clinopyroxenes in equilibrium with garnet in mafic granulites (Mazzuchelli et al. 1992). Clinopyroxene from websterite PBN 86-19 has high LREE content despite its high $Mg^{\#}$ (89) and low concentration of other trace elements. PBN 98-92 shows high REE, Ba, Rb and Nb concentrations but it has low Zr and Hf content. The major element composition of clinopyroxene and plagioclase are generally not correlated with their trace element contents (Fig. 5). The minerals are generally enriched in trace elements compared to theoretical cumulus phase content (see discussion section for detailed explanation). Some samples are strongly enriched in trace elements compared to the cumulus trend (PBN 98-92: 8.3 and 6.5 ppm La in plagioclase and clinopyroxene, respectively;

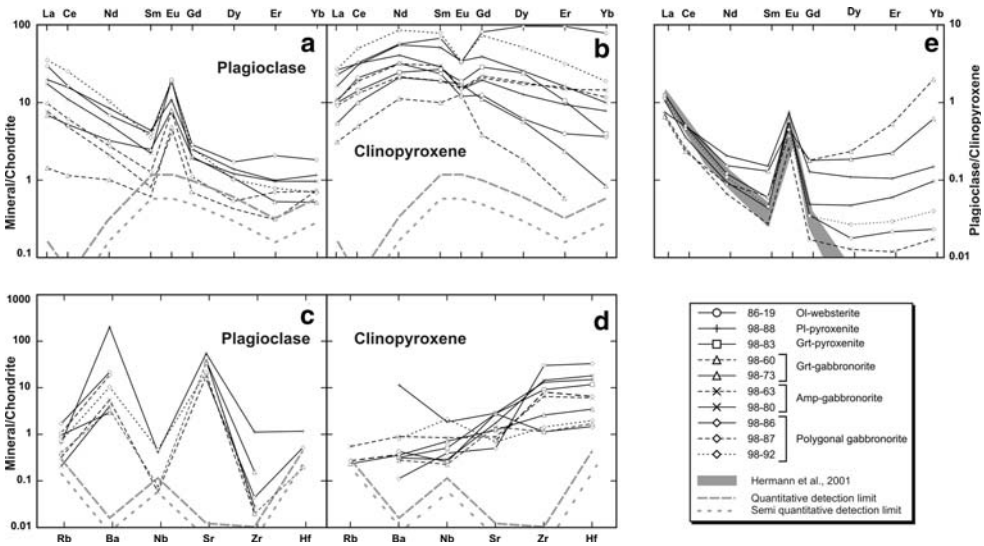

Fig. 4 REE patterns of plagioclase (**a**) and clinopyroxene (**b**). Trace element content of plagioclase (**c**) and clinopyroxene (**d**). Distribution coefficients of REE for plagioclase-clinopyroxene pairs (**e**). The grey area represent partition coefficient from Hermann et al. (2001)

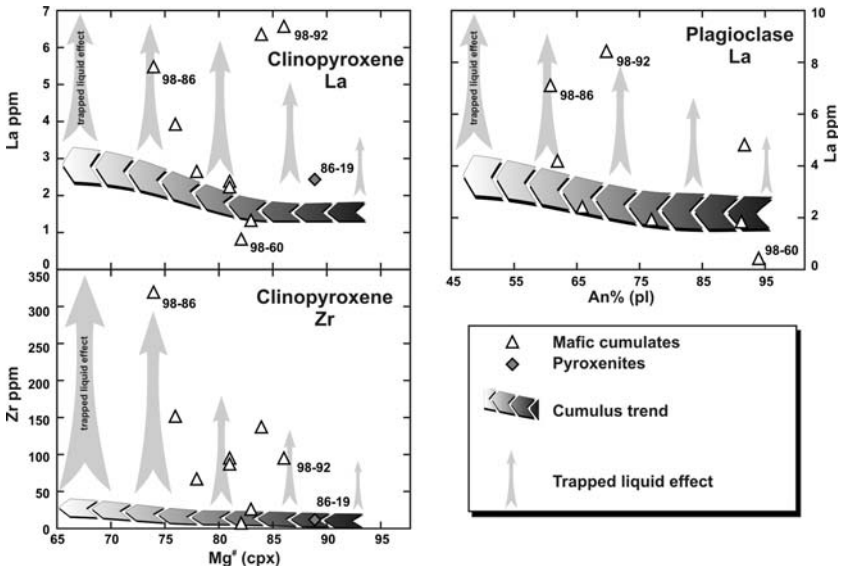

Fig. 5 Correlation between trace element contents and major elements of plagioclase (An%) and clinopyroxene ($Mg^{\#}$) of clinopyroxene. The cumulus trend represents the composition of phases in equilibrium with Late-Variscan Saar-Nahe volcanics (Schmidberger and Hegner 1999). Partition coefficients used in this calculation are from Hauri et al. (1994) for clinopyroxene and Bindeman et al. (1998) for plagioclase

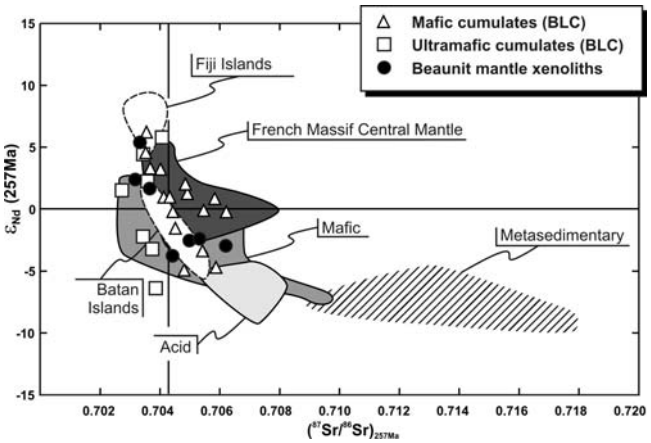

Fig. 6 Sr–Nd isotopic diagram for mantle and magmatic xenoliths from Puy Beaunit. The compositional fields of mantle, mafic, acid and metasedimentary xenoliths from French Massif Central are from Downes et al. (1990). Compositional fields of lavas and mantle xenoliths from Fiji and Batan Island are from Vidal et al. (1989)

PBN 98-86: 318 ppm Zr and 5.5 ppm La in clinopyroxene) whereas the minerals of PBN 98-60 and PBN 98-87 (0.3 and 2.3 ppm of La in plagioclase, respectively) plot on the cumulus trend.

Distribution coefficients between plagioclase and clinopyroxene are homogeneous for LREE and similar to those obtained for other deep-seated intrusions (Hermann et al. 2001) but variable for HREE (Fig. 4). In garnet-bearing xenoliths, the clinopyroxene has low HREE content which results in higher $K_d^{pl/cpx}$ values.

Whole-rock geochemistry

Sr–Nd isotopic geochemistry

Sr and Nd isotopic compositions (Fig. 6) have been measured on 35 samples (9 mantle peridotites and 26 ultramafic/mafic magmatic samples) and recalculated at 257 Ma, the SIMS zircon age obtained on a layered magmatic xenolith (Féménias et al. 2003). The $(\varepsilon_{Nd})_i$ and $(^{87}Sr/^{86}Sr)_i$ values for the mantle peridotites are in the range +5.3 to –3.8 and 0.7032–0.7062, respectively. These values are closely similar to those reported for present-day mantle xenoliths (Batan Island) and volcanics (Fiji islands) from island arcs (Vidal et al. 1989). The rather dispersed values observed in mantle xenoliths from Puy Beaunit argue for a heterogeneous upper mantle source that has been variously enriched by a crustal component, most probably during an early-Variscan subduction. The ultramafic and mafic magmatic xenoliths have similar isotopic compositions: $(\varepsilon_{Nd})_i$ is in the range +6.4 to –5.8 and +4.6 to –4.9, respectively, and $(^{87}Sr/^{86}Sr)_i$ ratios are between 0.7027–0.7041 and 0.7035–0.7062, respectively. The isotopic compositions of the mantle rocks and of the magmatic rocks largely overlap. This shows that the sampled upper mantle is the source of the parental magma of the BLC. The marked difference in isotopic compositions between magmatic xenoliths from Puy Beaunit and metasedimentary lower crustal xenoliths of the

French Massif Central (Downes et al. 1990) precludes significant amounts of crustal contamination during differentiation in the lowermost crust. This is also confirmed by the general absence of correlations between initial isotopic ratios and concentration of major and trace elements (Mg, K).

The range of isotopic composition of calc-alkaline acid (charnockites) meta-igneous xenoliths covers slightly the one of mafic/ultramafic xenoliths from Beaunit (Fig. 6); they are generally related to the mafic samples by an AFC process (Downes et al. 1990). It is not possible to study these xenoliths at Beaunit because they have been partially melted and contaminated in response to the transport by the host lava. However, the acid xenoliths from Beaunit could represent the crystallisation products of the most differentiated (and/or contaminated by crustal paragneiss) magma from the BLC complex.

Major element variations

Major element composition of magmatic ultramafic (pyroxenites and peridotites) and mafic samples has been plotted in binary MgO versus oxide diagrams (Fig. 7). Ultramafic samples have high MgO (>20 wt%), low Al_2O_3 (<5 wt%) and alkali (Na_2O < 0.6 wt%) contents which reflect the high proportion of Mg–Fe silicates (olivine and pyroxene) and the low modal proportions of aluminous phases. The SiO_2 content starts to increase with decreasing MgO in ultramafic cumulates to a maximum of 53 wt% in most evolved pyroxenites; it then dramatically decreases for mafic samples and can be as low as 39 wt% in garnet-bearing samples. The Al_2O_3 content is low (<3 wt%) and roughly equal for ultramafic samples, but it is quite high in gabbroic xenoliths (up to 25 wt%) due to the modal abundance of aluminous phases. CaO content progressively increases with decreasing MgO up to a maximum of 19 wt% in the plagioclase-clinopyroxenite. TiO_2 contents also progressively increase: ultramafic samples are TiO_2-poor (0–0.3 wt%) whereas mafic samples are characterised by 0.3–1.3 wt% TiO_2. The ilmenite-bearing garnet anorthosite is Ti-rich when compared to other samples (2.4 wt% of TiO_2).

Compositional evolution trends for magmatic xenoliths from Puy Beaunit have been compared to cumulates from a tholeiitic (Bushveld; Eales and Cawthorn, 1996) and a calc-alkaline (Cabo-Ortegal; Santos Zalduegui et al. 2002) plutonic complex. The Beaunit trends appear sometimes intermediate between the Bushveld and Cabo-Ortegal trends but several meaningful similarities with calc-alkaline cumulates from Cabo-Ortegal can be pointed out:

1. gabbroic rocks have high Al_2O_3 contents which suggest a strong Al-enrichment in the crystallising liquid;
2. there is a net decrease in SiO_2 (down to 39 wt%) for rocks with MgO < 20 wt%;
3. Na_2O content is roughly constant in the ultramafic rocks but dramatically increases in the mafic xenoliths. In contrast, tholeiitic cumulates from Bushveld show a progressive increase in Na_2O with decreasing MgO.

Trace element variations

Variations of trace element contents with MgO are illustrated for three elements with contrasting geochemical behaviour (Fig. 7): (1) Cr which is generally compatible in Fe–Mg silicates; (2) Sr which is compatible in plagioclase and (3) Zr which is a HFSE incompatible in most silicates. The Cr content is high in ultramafic samples (2000–3200 ppm and up to 5500 ppm in a Cr-spinel-bearing dunite) and below 1000 ppm for mafic samples. In contrast, Sr and Zr contents are low in ultramafic samples (Zr < 20 ppm; Sr < 100 ppm) and rapidly increase in mafic samples with MgO < 15 wt% (Zr: up to 100 ppm; Sr: up to 600 ppm). These variations are correlated with the sudden appearance of plagioclase and the disappearance of olivine in mafic samples.

Trace element abundances in the ultramafic magmatic samples have already been discussed in details by Féménias et al. (2003). The trace element signatures normalised to N-MORB (Hofmann 1988) are shown in Fig. 8. The main characteristics are: enrichment in LILE (Rb, Ba, K...), negative anomalies in Nb, Ta, Zr and Hf and positive anomalies in Pb. These features together with comparison with contemporaneous (Late Carboniferous-Permian) lavas point to a calc-alkaline affinity (Féménias et al. 2003).

The mafic samples share the same general features. They are enriched in LILE and LREE compared to HFSE (HREE included), they show positive anomalies in Ba, Sr and Pb (elements compatible or only slightly incompatible in plagioclase) and negative anomalies in P, Zr and Hf. Samples with low trace element content generally show a positive Ti anomaly whereas samples with high content of incompatible elements show no or a slight negative anomaly. In contrast with the magmatic peridotites and pyroxenites cumulates, the mafic cumulates do not show negative Nb–Ta anomalies. Some variations are observed between the different petrographical families:

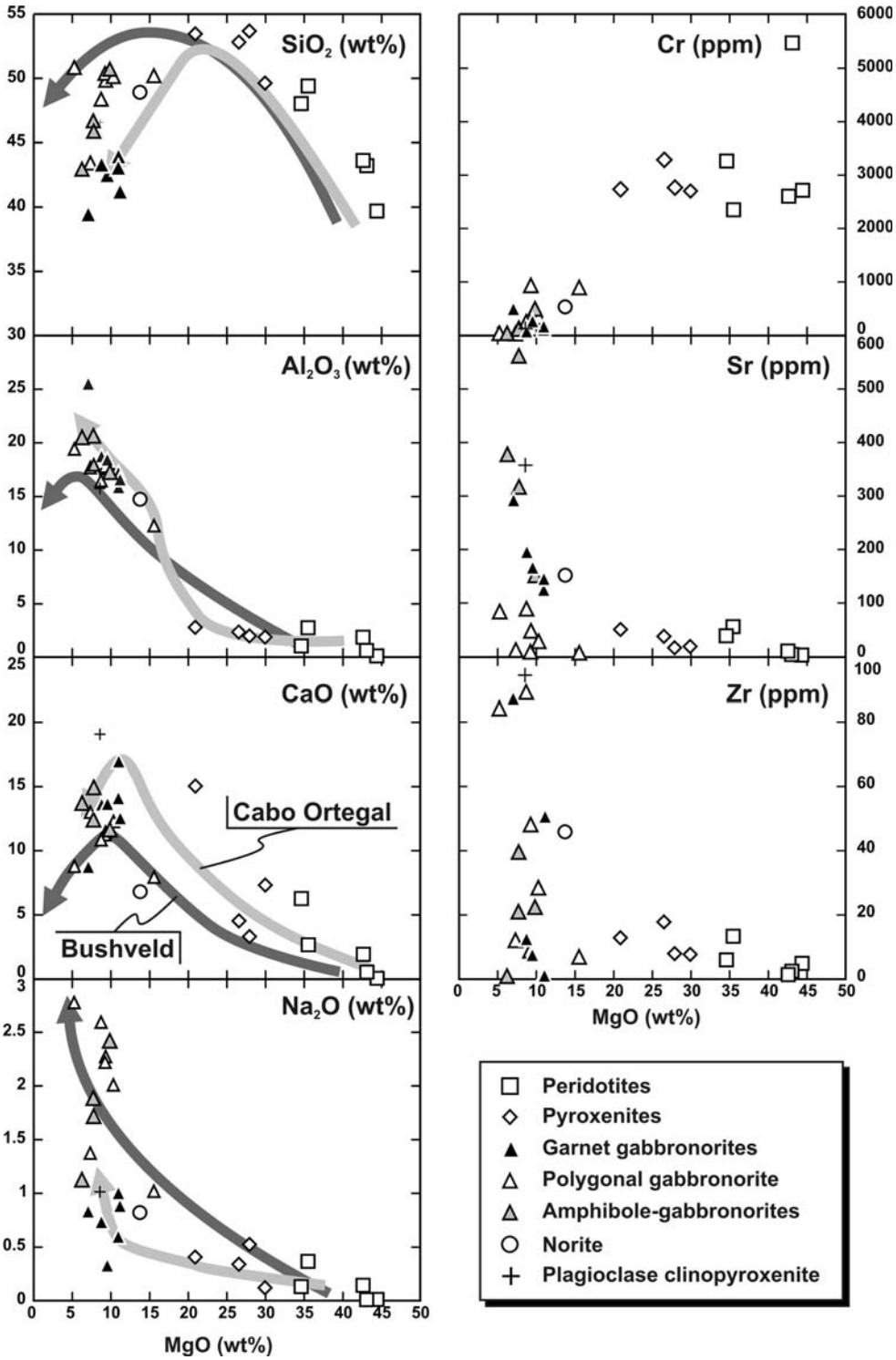

Fig. 7 Binary MgO versus oxide and MgO versus trace element diagrams for magmatic xenoliths from Puy Beaunit. The light grey arrow represent compositional trends in calc-alkaline arc root from Cabo Ortegal (Santos Zalduegui et al. 2002) and the dark grey arrow represent the trend of tholeiitic cumulates from Bushveld (Eales and Cawthorn 1996)

- rocks with euhedral garnet have higher HREE content ($Yb_N > 1$) than other samples ($Yb_N < 1$). This was the main argument to demonstrate that garnet was a cumulate phase in euhedral garnet-bearing gabbronorites (Berger et al. 2005). The garnet anorthosite with ilmenite (PBN 98-75) is also characterised by a strong positive Nb–Ta anomaly and higher Zr, Hf and Ti content. Enrichment in these elements is diagnostic of the presence of ilmenite as a cumulus phase (Green and Pearson 1987). The plagioclase-bearing garnet pyroxenite PBN 98-83, despite its low plagioclase content

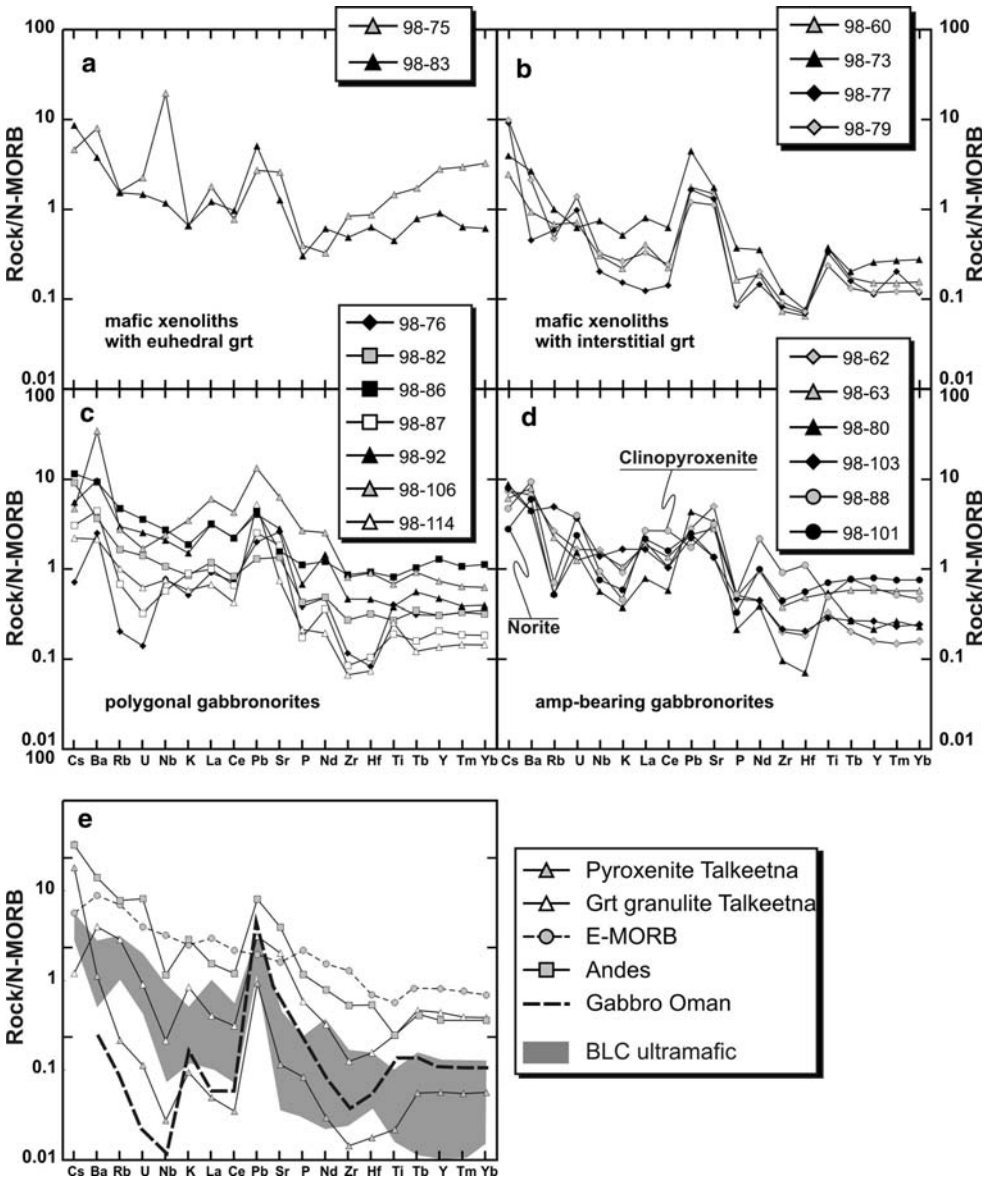

Fig. 8 Multi-elements diagrams normalised to N-MORB (Hofmann 1988) for mafic xenoliths with euhedral garnet (**a**); xenoliths with interstitial garnet (**b**); polygonal gabbronorites (**c**); amphibole-bearing gabbronorites with plagioclase pyroxenite PBN 98-88 and norite PBN 98-101 (**d**). The pattern of the ultramafic magmatic xenoliths (Fémémias et al. 2003); of calc-alkaline cumulates from Tonsina and of tholeiitic cumulate from Oman (Kelemn et al. 2004) and the pattern of typical E-MORB (Klein 2004) are shown for comparison (**e**)

(<1%), still shows a positive Pb anomaly but no Sr anomaly;

- mafic samples with anhedral interstitial garnet do not show the Ba anomaly but show a slight positive U anomaly;
- the fine-grained gabbronorite PBN 98-106 is relatively rich in trace-elements; it does not show a Sr anomaly but a slight positive Pb anomaly is present;
- the amphibole gabbronorites have a slight positive Ba anomaly coupled with a relative depletion in Rb and a strong negative P anomaly;
- the plagioclase-bearing clinopyroxenite is enriched in all trace elements and displays a negative anomaly in Pb and a slight depletion in K and Nb.

By comparison with other mafic rocks from well know tectonic settings (Fig. 7), the mafic xenoliths from Beaunit share similarities with both tholeiitic and calc-alkaline rocks: (1) they show LILE enrichment compared to N-MORB and tholeiitic rocks but lower that what is observed in fossil or active magmatic arcs; (2) there is no negative Nb–Ta anomalies like calc-alkaline rocks; (3) Pb anomaly is present in all samples, regardless of the modal proportion of plagioclase. This is a classical feature of calc-alkaline rocks.

Rare earth element variations

The chondrite-normalised (McDonough and Sun 1995) REE patterns are plotted in Figs. 9 and 10 according to their lithological group. The rocks with euhedral cumulus garnet (Berger et al. 2005) are characterised by HREE enrichment. The garnet anorthosite PBN

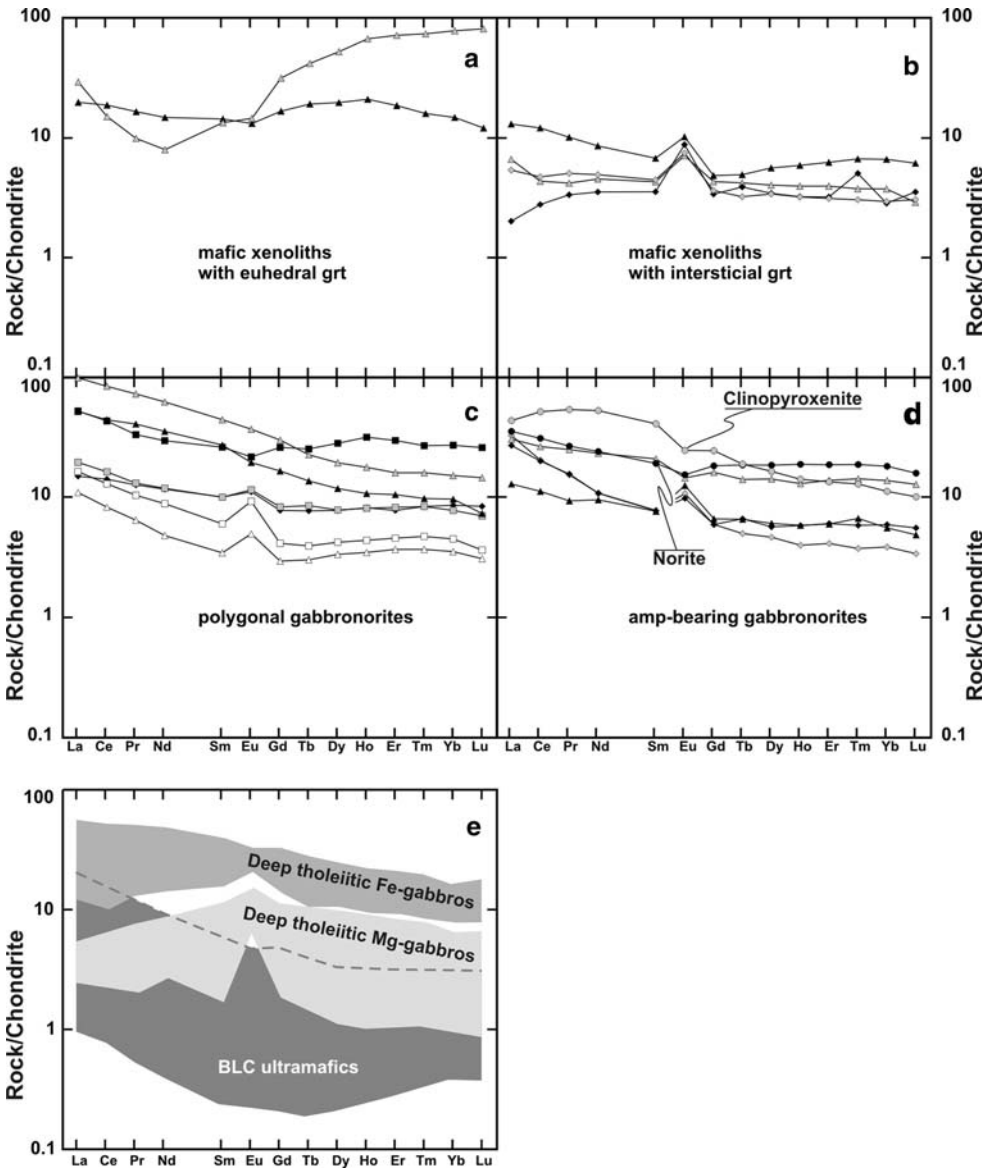

Fig. 9 REE patterns normalised to chondrites from McDonough and Sun (1995) for xenoliths with euhedral garnet (**a**); xenoliths with interstitial garnet (**b**); polygonal gabbronorites (**c**); amphibole-bearing gabbronorites with plagioclase pyroxenite PBN 98-88 and norite PBN 98-101 (**d**). The patterns of the ultramafic magmatic xenoliths (Fémények et al. 2003) and of tholeiitic Permian gabbros from crust-to-mantle transition zone (Hermann et al. 2001) are shown for comparison (**e**)

98-75 has a low $(Nd/Yb)_N$ value of 0.1 but shows a LREE enrichment ($(La/Nd)_N$ = 3.70) which is probably due to the high modal abundance of LREE-rich cumulus plagioclase and of significant amounts of trapped intercumulus liquid. Samples with anhedral garnet are LREE-enriched. They are also characterised by a strong positive Eu anomaly (Eu/Eu* = 1.65–2.53), typical of plagioclase cumulates. Gabbronorite PBN 98-77 is the only LREE-depleted sample ($(La/Yb)_N$ = 0.7) and it also has the lowest REE content (ΣREE = 8.14 ppm). PBN 98-73 shows a slightly convex upward parttern for HREE, this may be due to higher proportion of cumulus clinopyroxene (HREE-rich mineral compared to plagioclase).

Four polygonal gabbronorites are LREE-enriched with a positive Eu anomaly, due to accumulation of plagioclase. Sample PBN 98-86 has an almost flat pattern with a slightly negative Eu anomaly and a significant enrichment in HREE compared to LREE. The two fine-grained gabbronorites (PBN 98-92 and PBN 98-106) are REE rich (ΣREE = 75.15–136.84 ppm) with a strong LREE-enrichment ($(La/Yb)_N$ = 5.38–6.51) and no Eu anomaly. The presence of minor proportion of apatite in PBN 98-106 could explain this REE distribution but this sample is also enriched in most trace elements and has the most evolved mineral composition (An_{48}; $Mg^{\#}$ of cpx: 65). From a geochemical point of view, it probably corresponds to a magmatic melt and not to a cumulate. In contrast, PBN 98-92 does not contain apatite (P_2O_5: 0.08 wt%) and has pyroxenes with high $Mg^{\#}$ (cpx: 85–88; opx: 76). These features could result from high modal propor-

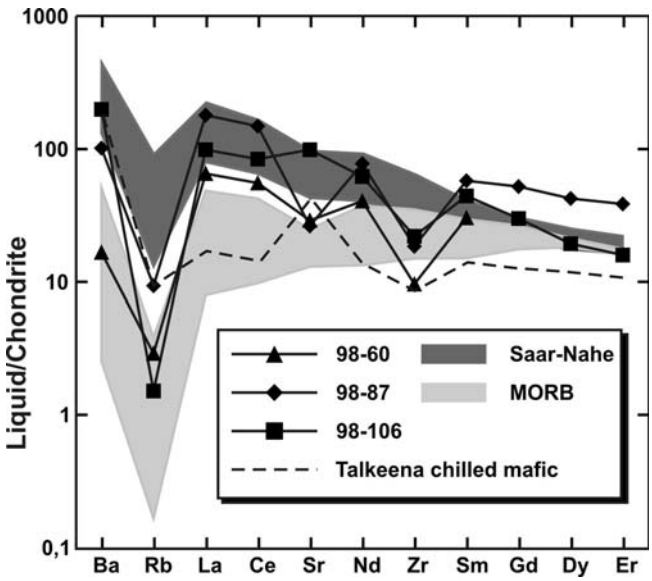

Fig. 10 Trace element patterns of liquids in equilibrium with the most primitive clinopyroxenes from Puy Beaunit mafic xenoliths. Whole-rock composition of chilled gabbronorite PBN 98-106 is shown for comparison. Compositional field of MORB from (Klein 2004) and composition of Saar-Nahe volcanics from Schmidberger and Hegner (1999)

tion of intercumulus liquid in a primitive cumulate (Barnes 1986; Hermann et al. 2001).

Three amphibole-bearing mafic xenoliths are also characterised by positive Eu anomalies and LREE-enrichment due to plagioclase accumulation. The pyroxene-rich amphibole gabbronorite PBN 98-63 and norite PBN 98-101 also show LREE-enrichment but they have small negative Eu anomaly (Eu/Eu* = 0.79–0.82). They could correspond either to more differentiated cumulates or to samples with a higher proportion of residual interstitial liquid with a negative Eu anomaly. The plagioclase-clinopyroxenite PBN 98-88 has a REE distribution that mimics those of clinopyroxenes: i.e., a convex LREE pattern and a slight negative Eu anomaly. The whole-rock REE content is here controlled by cumulus clinopyroxene.

Gabbros from a deep-seated tholeiitic intrusion (Hermann et al. 2001) are generally LREE-depleted except for some Fe-rich gabbros the magmatic mafic and ultramafic xenoliths from Puy Beaunit are LREE-enriched even compared with samples expected as pure cumulates (low trace elements contents and primitive major element composition). This could be a feature of the parental liquid.

Discussion

Enriched sub-alkaline magma as a parental melt for the Beaunit layered complex

Sr–Nd isotopic data from Beaunit magmatic and mantle xenoliths demonstrate the co-genetic character of the whole mafic and ultramafic cumulates. Indeed, the data significantly overlap for the different magmatic rocks and no significant difference is observed between ultramafic and mafic cumulates. The magmatic xenoliths are thought to represent pieces of a deep-seated layered intrusion here called the BLC. However, the composition of the parental melt is still unclear. Indeed, as the Beaunit xenoliths from this study are mainly cumulates, we cannot directly have information about the parental melt composition.

The mafic magmatic xenoliths are characterised by the presence of igneous Ti-amphibole (up to 20%) and garnet (up to 30%). Magmatic amphibole is a major phase in calc-alkaline gabbros, where it plays a crucial role in differentiation processes (Foden and Green 1992) but it can also be present in tholeiitic deep cumulates (Tribuzio et al. 2000; Desmurs et al. 2002). On the other hand, igneous garnet is only observed in natural calc-alkaline rocks (see discussion in Harangi et al. 2001). It crystallise in response to a strong Al enrichment of the hydrated magma at high pressure (around 1 GPa and higher; Green and Ringwood 1968; Harangi et al. 2001; Muntener et al. 2001). In contrast, garnet crystallisation in tholeiitic magma is generally effective at higher pressures (>1.2 GPa, Green and Ringwood 1968).

LILE- and LREE-enrichments are observed in all mafic and ultramafic samples whereas deep-seated tholeiitic gabbros are generally LREE-depleted (Fig. 8; Hermann et al. 2001). These geochemical characteristics were thus probably inherited from the parental magma and not from fractional crystallisation processes. The same features characterise calc-alkaline lavas and their related mafic-ultramafic cumulates (Fig. 7) whereas tholeiitic gabbros and lavas generally

show low LILE contents (Klein 2004). However, Nb–Ta negative anomalies are absent in mafic samples. This characteristic is one of the major fingerprint of the calc-alkaline magma whereas they are absent in tholeiitic series. Moreover, the fine-grained gabbronorite PBN 98-106 ($Mg^{\#}$: 47) has a LREE-enriched pattern (with no Eu anomaly) and high trace elements content. From a geochemical point of view, it is a liquid, not a cumulate. It falls just at the transitional zone in a AFM diagram and within the tholeiitic field in FeO/MgO versus SiO_2 diagram but within the field of most primitive calc-alkaline lava from Mt-Shasta (Grove et al. 2003). Sr–Nd isotope geochemistry also demonstrates the enriched characteristic of the mantle source of BLC parental melt. The source is a former mantle wedge variously enriched by Variscan subduction and depleted during active margin magmatism. This observation fits well with the pertographic and geochemical characteristic of the Beaunit mantle xenoliths (presence of hydrous phases and enriched geochemical fingerprint; Féménias et al. 2004). Indeed, mantle sources with similar isotopic compositions have been proposed for lavas from subduction zones (Vidal et al. 1989; Fig. 5).

To clarify the geochemical affinity of the parental melt of the BLC, we have calculated the liquid in equilibrium with clinopyroxene and plagioclase from some chosen rocks using the partition coefficient of Hauri et al. (1994) and Bindemann et al. (1998). As no primitive clinopyroxene has been analysed (Mg-rich and low trace elements content), we will have to choose sample that already undergone differentiation. However, this would give us information on the liquid composition. The layered mafic cumulate PBN 98-60 has rather primitive mineral major elements composition ($Mg^{\#}$ of cpx: 82, An% of plagioclase: 94) but also shows low trace element contents in whole rock and in minerals. LILE (Ba, Rb, Sr) content of the equilibrium liquid has been estimated using plagioclase composition and HFSE (REE, Zr) contents were estimated using clinopyroxene composition. Unfortunately, as the clinopyroxene from sample PBN 98-60 has been re-equilibrated with garnet, its HREE content has been modified and we cannot calculate the HREE composition of the liquid. Plagioclase and clinopyroxene from the gabbronorite PBN 98-87 have also low trace elements contents and they can give some information about the crystallising liquid. The most primitive calculated liquid (from PBN 98-60) is intermediate to enriched tholeiitic liquids (E-MORB, Klein 2004) and to Saar-Nahe calc-alkaline lava. It shows intermediate REE contents (between 10 and 100x the chondrites) with significant LREE enrichment and a pronounced negative anomaly in Rb. The liquid calculated from PBN 98-87 has a sub-parallel profile but it is richer in trace elements and shows a negative Sr anomaly. This probably a more differentiated liquid which has already fractionated plagioclase. When compared to the two calculated liquids, the whole-rock trace element composition of the fine grained gabbronorite PBN 98-106 looks rather similar, it has a sub-parallel trace element pattern with intermediate LILE and LREE contents; the only significant difference is the greater content in HREE. This also demonstrates that PBN 98-106 is probably a chilled mafic rock and not a cumulate. Calculated liquids from the BLC also significantly differs from calc-alkaline arc magma as exemplified by the Talkeena mafic cumulates (Greene et al. 2006). Such magmas always show strong negative Nb–Ta anomalies, flat or only slightly enriched LREE patterns and generally lower REE contents. The mantle source of the BLC parental magma is different from true arc mantle wedge. Indeed, the mantle source in Beaunit has been reactivated 100 Ma after the subduction-related enrichment and has already been depleted during Devonian active margin magmatism.

All the previous observations argue for a transitional enriched sub-alkaline magma as the parental melt of the BLC. Indeed, the mafic cumulates from the BLC share similarities with both tholeiitic and calc-alkaline series. This transitional characteristic could be explained by the complex history of the sub-continental mantle beneath Puy Beaunit during Variscan times. The mantle has indeed been enriched by a subduction event during eo-variscan times (before 360 Ma; Féménias et al. 2004) and it has also undergone two partial melting episode: (1) in response to mantle hydration during subduction (active margin magmatism before Carboniferous) and (2) in response to adiabatic decompression during Late-Variscan transcurrent tectonics (Féménias et al. 2004). The melt produced during this last event has crystallised the cumulates from the Permian BLC. The mantle source of the BLC has most probably lost a part of its ‘‘enriched’’ component during the first Devonian melting event. This is the reason why the BLC cumulates does not show classical negative Nb–Ta anomalies and why the composition of calculated equilibrium liquids is intermediate between enriched tholeiitic magma (E-MORB) and subduction-related calc-alkaline lava (Saar-Nahe). The first depletion and the high degrees of partial melting also explain why the second melting event has generated high-Mg basalts (see below) as parental magma of the BLC (Féménias et al. 2004).

Fractional crystallisation at high pressure

The most primitive cumulates are peridotites: they are rich in olivine and they have Fe–Mg silicates with the highest $Mg^{\#}$. These cumulates most probably crystallised from a high-Mg basalt because natural primitive basalts and andesites crystallise liquidus olivine around 1 GPa only if the liquid is enriched in MgO (Müntener et al. 2001). Assuming a $K_D^{Fe/Mg}$ between olivine and liquid of 0.32 at 1.2 GPa for hydrous melts (Ulmer 1989), the most primitive olivine (Fo_{90}) would have crystallised from a magma with a $Mg^{\#}$ of 74. The abundance of cumulus olivine and of Fe–Cr–Al spinel in ultramafic xenoliths precludes a parental magma with high-SiO_2 content (>52 wt%). Indeed, Si-rich, Mg-poor basalts or basaltic andesites generally crystallise pyroxenites as most primitive cumulates rather than peridotites at pressure corresponding to the lowermost crust (Muntener et al. 2001; Grove et al. 2003). The parental magma of the BLC was probably a high-Mg basalt with relatively low-SiO_2 as also confirmed by partial melting modelling on mantle xenoliths (Fémémias et al. 2004).

Intense crystallisation of Al-poor phases (olivine, pyroxenes, Cr-spinel) steadily increased the Al-content of the BLC magma leading to strong Al enrichment. This is shown by the increasing Al-content of clinopyroxene with decreasing $Mg^{\#}$ (assuming constant lithostatic pressure during differentiation) up to a maximum of 0.35 Al p.f.u. (7.8 wt% Al_2O_3) in the garnet-bearing plagioclase pyroxenite. The Al-rich cumulates fractionated afterwards from high-alumina basalt. This is confirmed by the presence of magmatic garnet which is the evidence of high-alumina-basalt fractionation at pressure around 1 GPa (Harangi et al. 2001). The absence of amphibole in ultramafic assemblage and the lack of hornblendites argue for rather low water content of the magma (≤4%) at P ≈ 1 GPa (Foden and Green 1992; Muntener et al. 2001; Ulmer et al. 2003).

Consequently, mafic cumulates are dominated by An-rich plagioclase, pyroxenes, garnet and amphibole with a lower proportion of pyroxenes than in ultramafic cumulates. Chemically, they are characterised by low-SiO_2 and high-Al_2O_3 contents with sometimes very low $Mg^{\#}$. For example, the ilmenite-bearing garnet anorthosite (PBN 98-75: SiO_2: 39 wt%; Al_2O_3: 25 wt%; An% of plagioclase: 93) has a low $Mg^{\#}$ (44) whereas high-Al basalts have generally $Mg^{\#} > 50$ (Kelemen et al. 2004). In our case, the clinopyroxenes ($Mg^{\#}$: 75–85) from high-Al cumulates give equilibrium liquids with $Mg^{\#}$ in the range of 48–61, considering a $K_D^{Fe/Mg}$ of 0.3 at 1 GPa (Muntener et al. 2001). Crystallisation of low-Mg cumulates could increase the $Mg^{\#}$ of the magma during differentiation. This process is presumably uncommon; however, it could form rare garnet- and oxide-rich cumulates (only one xenolith from Puy Beaunit).

Fractionation of Al-Ca-rich and SiO_2-poor cumulates has lead to Si-enrichment and Al-depletion in the liquid during differentiation. This is shown by the low-Al content of pyroxenes with low $Mg^{\#}$ (Fig. 2). However, the melt in equilibrium with the most evolved clinopyroxene ($Mg^{\#}$: 65) still had a relatively high $Mg^{\#}$ (37); its SiO_2 content was probably quite low (55–60 wt% SiO_2, following evolution trends in sub-alkaline magmas from Grove and Baker (1984). Cumulates at this stage have generally high SiO_2 (up to 52%); they are represented by polygonal gabbronorites.

Several difficulties arise when trying to quantify the fractional crystallisation process for BLC because several important parameters cannot be reasonably estimated: (1) the composition of parental liquid in equilibrium most primitive clinopyroxene cannot be estimated because there is no ''primitive'' clinopyroxene with both high $Mg^{\#}$ and low trace element contents. The enrichment in incompatible elements observed in most magnesian pyroxenes is probably due to re-equilibration of cumulus minerals with significant amounts of intercumulus liquid (see below); (2) it is not realistic to model fractional crystallisation assuming constant bulk $D_{rock/melt}$ because in Beaunit, modal composition of cumulates vary largely during fractional crystallisation; (3) the relative proportions of the various lithologies at depth obviously cannot be evaluated because the BLC is sampled as xenoliths. Without reasonable estimations of these parameters, quantitative modelling would be highly speculative.

Controls on trace-elements abundances

Two main parameters control the trace element abundance in cumulates: the nature of the cumulus phases and the amount of trapped interstitial liquid. The effect of this liquid on the composition of cumulus minerals is illustrated on Fig. 4. The cumulus trend represents the composition of the theoretical cumulus phase (plagioclase or clinopyroxene) in equilibrium with basaltic to andesitic lavas from Saar-Nahe (Schmidberger and Hegner 1999), calculated with the partition coefficients of Hauri et al. (1994) for clinopyroxene and Bindeman et al. (1998) for plagioclase. The Saar-Nahe lavas were erupted in the same tectonic setting as the BLC; they have the same trace element distribution as ultramafic cumulates and are thus good analogues of the BLC rocks. Most analysed

minerals from Beaunit xenoliths plot above the cumulus trend and are enriched in trace element compared to the theoretical cumulus composition for a given $Mg^{\#}$ or An content. This is interpreted as the effect of re-equilibration of the cumulus phases with the interstitial liquid. Indeed, in slowly cooled cumulates, the trapped interstitial liquid exchanges its trace elements with the cumulus minerals. Barnes (1986) (and later Cawthorn 1996 and Hermann et al. 2001 for deep cumulates) demonstrated that the ''trapped liquid shift'' causes an enrichment of the trace elements contents of cumulus minerals while major element composition varies only slightly. These data also demonstrates that there is no valuable ''primitive'' clinopyroxene that can be used to calculate the composition of the parental liquid of the BLC. The most magnesian clinopyroxene are enriched in trace elements (e.g. PBN 86-19, $Mg^{\#}$: 89) and some clinopyroxene have low trace element contents but are enriched in iron (e.g. PBN98-60, $Mg^{\#}$: 82). The minerals of gabbronorites PBN 98-86 and 98-92 are strongly enriched in trace elements despite their relatively high $Mg^{\#}$ (74 and 86, respectively); this demonstrate that the cumulus clinopyroxene from these samples have been requilibrated with intercumulus liquid during cooling of the BLC. Moreover, the whole-rocks are also enriched in REE and do not show a positive Eu anomaly (Fig. 8) despite the high modal proportion of plagioclase (>50%).

The whole-rock trace element patterns are strongly controlled by cumulus minerals. Plagioclase cumulates have LREE-enrichment with high contents of Eu, Ba, Sr and Pb. Clinopyroxene cumulates have high REE content with low Eu and Ba and high HFSE contents. Garnet cumulates are mainly characterised by a strong HREE-enrichment. Rare ilmenite-rich cumulates show low-SiO_2 with high Ti, Nb and Ta contents. Sr and Nd initial isotopic ratio do not show any correlation with elements enriched (K) or depleted (Mg) in the metasedimentary lower crust. It thus demonstrates that crustal contamination has not played an important role for trace element distribution in the BLC cumulates.

Evidence for a heterogeneous crust-mantle transition zone beneath the French Massif Central

The suite of ultramafic-mafic xenoliths from Beaunit derives from a Permian deep layered intrusion (BLC, Féménias et al. 2003). The latter was formed during a late-Variscan tectono-magmatic event that generated widespread magmatic activity of tholeiitic and calc-alkaline affinity throughout western Europe. The BLC is younger than the main granulite facies metamorphic event of Carboniferous age (Downes et al. 1990) because it did not register this late-Variscan HT episode (Berger et al. 2005). Leyreloup (1974) pointed out that such preserved magmatic xenoliths (devoid of Carboniferous granulitic metamorphism, including Beaunit ultramafic/mafic xenoliths) are uncommon in the French Massif Central and are only found in the northern part of the Chaîne des Puys, close to a major late-Variscan fault (Blansy-Le Creusot fault). Moreover, the Permian (late-Variscan) volcanism in French Massif Central is restricted to large transcurrent strike slip faults and related pull-apart basins (see references in Féménias et al. 2003). We propose that the lower crustal rocks devoid of pervasive granulitic metamorphism such as the magmatic xenoliths from Beaunit are restricted to the root zones of strike-slip faults still active during Permian.

The lowermost crust in the northern part of Chaîne des Puys, close to Beaunit area, is characterised by higher *P*-wave velocity (6.9–7.0 km/s; Zeyen et al. 1997). Moreover, an ''anomalous mantle'' has been detected in the same area at 25–30 km depth; it is characterised by low *P*-wave velocity of 7.2–7.5 km/s that gradually increases to typical upper mantle values (8–8.4 km/s; Perrier and Ruegg 1973; Zeyen et al. 1997). This anomaly leads to confusing interpretation for the depth of Moho close to Beaunit. However, recent experimental work has shown that mafic and ultramafic plutons in the deep crust can have densities close to residual mantle value (Muntener et al. 2001), implying that they have comparable *P*-wave velocity at a given temperature. In other intra-continental areas, such features have been directly interpreted as mafic/ultramafic cumulates underplating the metamorphic crust (DEKORP-BASIN Res. Group 1999). At Beaunit, mafic xenoliths crystallised at about 1 GPa (30 km depth); we thus interpret the low velocity zone below northern part of Chaine des Puys as the mafic/ultramafic intrusion from which the xenoliths derive. This view of the Moho discontinuity beneath northern French Massif Central agrees with the model proposed by Griffin and O'Reilly (1987) and Chen et al. (2001) of a gradual transition from crustal mafic/ultramafic rocks to residual upper mantle peridotites.

Conclusion

The ultramafic-mafic xenoliths from Puy Beaunit are derived from a Permian deep (30 km depth) intrusion called the BLC. The compositional evolution of cumulates can be related to fractional crystallisation of a mantle-derived melt without significant amount of

crustal contamination. The ultramafic cumulates dominated by peridotites and pyroxenites have crystallised from primary high-Mg basalts. Fractionation of Al-poor phases (olivine and pyroxenes) has progressively enriched the melt in Al. Saturation in Al of the crystallising liquid enhanced the accumulation of Si-poor, Al-rich phases to form aluminous garnet- and amphibole-bearing gabbronorites. The most evolved cumulates are gabbronorites; they were derived from a basaltic to andesitic magma. This study demonstrates that even under high pressure of crystallisation, olivine can still be a liquidus phase in a high-Mg magma with rather low water content (~3 wt%). Ultramafic cumulates show strong calc-alkaline affinity and mafic cumulates show transitional characters between tholeiitic and calc-alkaline series.

The particular location of the Puy Beaunit, above a fertile mantle and close to a major fault active during Permian times, explains why the mafic/ultramafic xenoliths from Beaunit are exceptional compared to the suite of late-Variscan granulitic xenoliths in the FMC. Indeed, the xenoliths are devoid of pervasive granulite facies recrystallisation and the mafic xenoliths are clearly associated with ultramafic cumulates. The presence of ultramafic-mafic cumulates at 30 km depth is evidence that the low velocity zone below the seismic Moho is probably not pure abnormal mantle. This zone could either correspond to lower crustal intrusions of underplated magma or to cumulates interlayered with upper mantle.

Acknowledgments Othmar Müntener is thanked for its complete and constructive review of a first draft of the present paper. The comments of Hilary Downes helped to clarify the manuscript. Luc Andre is acknowledged for giving us access to LA-ICP-MS facilities.

References

Ashwall LD, Demaiffe D, Torsvik TH (2002) Petrogenesis of neoproterozoic granitoids and related rocks from the Seychelles: the case for an Andean-type arc origin. J Petrol 43:45–83

Barnes SJ (1986) The effect of trapped liquid crystallisation on cumulus mineral compositions in layered intrusions. Contrib Mineral Petrol 93:524–531

Baudry D, Camus G (1970) Les maars de la chaîne des Puys (formations volcaniques du Massif central français). Bull Soc Geol de France 12:185–189

Berger J, Féménias O, Coussaert N, Demaiffe D (2005) Magmatic garnet-bearing mafic xenoliths (Puy Beaunit, French Massif Central): P-T path from crystallisation to exhumation. Eur J Min 17:687–701

Bindeman IN, Davis AM, Drake MJ (1998) Ion microprobe study of plagioclase-basalt partition experiments at natural concentration levels of trace elements. Geochim Cosmochim Acta 62:1175–1193

Bishop FC (1980) The distribution of Fe^{2+} and Mg between coexisting ilmenite and pyroxene with applications to geothermometry. Am J Sci 280:46–77

Bologne G, Duchesne J-C (1991) Analyse des roches silicatées par spectrométrie de fluorescence X: précision et exactitude. Bel Geol Surv Prof Pap 249:1–11

Brousse R, Rudel A (1964) Bombes de péridotites, de norites, de charnockites et de granulites dans les scories du Puy Beaunit. C R Acad Sci Paris IIA 259:185–188

Camus G (1975) La Chaîne des Puys. Etude structurale et volcanologique. Thèse Doct Etat, Univ Clermont-Ferrand II, p 321

Cawthorn RG (ed) (1996) Layered intrusions. Elsevier, Amsterdam, p 531

Cawthorn RG, O'Hara MJ (1976) Amphibole fractionation in calc-alkaline magma genesis. Am J Sci 276:309–329

Chen SH, O'Reilly SY, Zhou XH, Griffin WL, Zhang G, Sun M, Feng JL, Zhang M (2001) Thermal and petrological structure of the lithosphere beneath Hannuoba, Sino-Korean Craton, China: evidence from xenoliths. Lithos 56:267–301

DEKORP-BASIN Res. Group (1999) Deep crustal structure of the Northeast German basin: Neao DEKORP-BASIN'96 deep-profiling results. Pure Appl Geophys 27:55–58

Desmurs L, Müntener O, Manatschal G (2002) Onset of magmatic accretion within magma-poor passive margins: A case study from the Err-Platta ocean-continent transition, Eastern Switzerland. Contrib Mineral Petrol 144:365–382

Downes H (1993) The nature of the lower continental crust of Europe: petrological and geochemical evidence from xenoliths. Phys Earth Planet Int 79:195–218

Downes H, Dupuy C, Leyreloup AF (1990) Crustal evolution of the Hercynian belt of Western Europe: Evidence from lower-crustal granulitic xenoliths (French Massif Central). Chem Geol 83:209–231

Eales HV, Cawthorn RG (1996) The Bushveld complex. In: Cawthorn RG (ed) Layered intrusions, developments on petrology, vol 15. Elsevier, Amsterdam, pp 181–229

Faure F, Trolliard G, Montel J-M, Nicollet C (2001) Nanopetrographic investigation of a mafic xenolith (maar de Beaunit, Massif Central, France). Eur J Mineral 13:27–40

Féménias O, Mercier J-CC, Demaiffe D (2001) Petrology of ultramafic xenoliths from the Puy Beaunit (French Massif Central): an unusual occurrence for the sub-continental mantle. C R Acad Sci Paris IIA 332:535–542

Féménias O, Coussaert N, Bingen B, Whitehouse M, Mercier J-CC, Demaiffe D (2003) A Permian underplating event in late- to post-orogenic tectonic setting: Evidence from the mafic-ultramafic layered xenoliths from Beaunit (French Massif Central). Chem Geol 199:293–315

Féménias O, Coussaert N, Berger J, Mercier J-CC, Demaiffe D (2004) Metasomatism and melting history of a Variscan lithospheric mantle domain: Evidence from the Puy Beaunit xenoliths (French Massif Central). Contrib Mineral Petrol 148:13–28

Féménias O, Ohnenstetter D, Coussaert N, Berger J, Demaiffe D (2005) Origin of micro-layering in a deep magma chamber: evidence from two ultramafic-mafic layered xenoliths from Puy Beaunit (French Massif Central). Lithos 83:347–370

Foden JD, Green DH (1992) Possible role of amphibole in the origin of andesite: some experimental and natural evidence. Contrib Mineral Petrol 109:479–493

Green DH, Ringwood AE (1968) Origin of garnet phenocrysts in calc-alkaline rocks. Contib Mineral Petrol 18:162–174

Green TH, Pearson NJ (1987) An experimental study of Nb and Ta partitioning between Ti-rich minerals and silicate liquids

at high pressure and temperature. Geochim Cosmochim Acta 51:55–62
Greene AR, DeBari SM, Kelemen PB, Blusztajn J, Clift PD (2006) A detailed geochemical study of Island arc crust: the Talkeetna arc section, South-Central Alaska. J Petrol 47:1051–1093
Griffin WL, O'Reilly SY (1987) Is the continental Moho the crust/mantle boundary? Geology 15:241–244
Grove TL, Baker MB (1984) Phase equilibrium controls on the tholeiitic versus calc-alkaline differentiation trends. J Geophys Res 89:3253–3274
Grove TL, Elkins-Tanton LT, Parman SW, Chatterjee N, Müntener O, Gaetani GA (2003) Fractional crystallization and mantle-melting controls on calc-alkaline differentiation trends. Contrib Mineral Petrol 145:515–533
Harangi Sz, Downes H, Kósa L, Szabó Cs, Thirlwall MF, Mason PRD, Mattey D (2001) Almandine garnet in calc-alkaline volcanic rocks of the northern Pannonian basin (Eastern-Central Europe): geochemistry, petrogenesis and geodynamic implications. J Petrol 42:1813–1843
Hauri EH, Wagner TP, Grove TL (1994) Experimental and natural partitioning of Th, U, Pb and other trace elements between garnet, clinopyroxene and basaltic melts. Chem Geol 117:149–166
Hermann J, Müntener O, Günther D (2001) Differentiation of mafic magma in a continental crust-to-mantle transition zone. J Petrol 42:189–206
Hill E, Wood BJ, Blundy JD (2000) The effect of Ca-Tschermaks component on trace element partitioning between clinopyroxene and silicate melt. Lithos 53:203–215
Hofmann AW (1988) Chemical differentiation of the Earth: the relationship between mantle, continental crust, and oceanic crust. Earth Planet Sci Lett 90:297–314
Jull M, Kelemen PB (2001) On the conditions for lower crustal convective instability. J Geophys Res 106:6423–6446
Kelemen PB, Hanghoj K, Greene AR (2004) One view of the geochemistry of subduction-related magmatic arcs, with an emphasis on primitive andesite and lower crust. In: Rudnick RL (ed) Treatise on geochemistry, vol 3, the crust. Elsevier, Pergamon, pp 593–659
Klein EM (2004) Geochemistry of the igneous oceanic crust. In: Rudnick RL (ed) Treatise on geochemistry, vol 3, the crust. Elsevier, Pergamon, pp 433–464
Leyreloup AF (1974) Les enclaves catazonales remontées par les éruptions néogènes de France: nature de la croûte inférieure. I. Lithologie et structurologie d'ensemble du complexe granulito-charnockitique sous-jacent au Massif Central français d'après les enclaves remontées par les volcans néogènes. Contrib Mineral Petrol 46:17–27
Mazzucchelli M, Rivalenti G, Vannucci R, Bottazzi P, Ottolini L, Hofmann AW, Sinigoi S, Demarchi G (1992) Trace element distribution between clinopyroxene and garnet in gabbroic rocks of deep crust: An ion microprobe study. Geochim Cosmochim Acta 56 2371:2385
McDonough WF, Sun SS (1995) The composition of the Earth. Chem Geol 120:223–253
Miyashiro A (1974) Volcanic rock series in island-arcs and active continental margins. Am J Sci 274:321–355
Müntener O, Kelemen PB, Grove TL (2001) The role of H_2O during crystallisation of primitive arc magmas under uppermost mantle conditions and genesis of igneous pyroxenites : an experimental study. Contrib Mineal Petrol 141:643–658
Perrier G, Ruegg J-C (1973) Structure profonde du Massif central francais. Ann Géophys 29:435–502
Rosseel J-B (1996) Synthèse chrono-magmatologique de la Chaîne des Puys. Unpublished diploma thesis (DEA), Univ B Pascal, Clermont-Ferrand II, 50 pp
Rudnick RL, Fountain DM (1995) Nature and composition of the continental crust a lower crustal perspective. Rev Geophys 33:267–309
Santos Zalduegui SF, Schärer U, Gil Ibarguchi JI, Girardeau J (2002) Genesis of pyroxenite-rich peridotite at Cabo Ortegal (Spain). Inferences from geochemical, mineral and Pb-Sr isotopic data. J Petrol 43:17–43
Schmidberger S, Hegner E (1999) Geochemistry and isotope systematics of calc-alkaline volcanic rocks from the Saar-Nahe basin (SW Germany). Implications for Late Hercynian orogenic development. Contrib Mineral Petrol 135:373–385
Singh SC, McKenzie D (1993) Layering in the lower crust. Geophys J Int 113:622–628
Sisson TW, Grove TL (1993) Experimental investigations of the role of H_2O in calc-alkaline differentiation and subduction zone magmatism. Contrib Mineral Petrol 113:143–166
Tribuzio R, Tiepolo M, Thirlwall MF (2000) Origin of titanian pargasite in gabbroic rocks from the Northern Apennine ophiolites (Italy): insights into the late-magmatic evolution of a MOR-type intrusive sequence. Earth Planet Sci Lett 176:281–293
Ulmer P. (1989) The dependence of the Fe^{2+}–Mg cation-partitioning between olivine and basaltic liquid on pressure, temperature and composition. Contrib Mineral Petrol 101:261–273
Ulmer P, Muentener O, Alonso Perez R (2003) Potential role of garnet fractionation in H_2O-undersaturated andesite liquids at high pressure: an experimental study and a comparison with the Kohistan Arc. Geophys Res Abstr 5:08308
Upton B, Aspen P, Hinton R (2001) Pyroxenite and granulite xenoliths from beneath the Scottish Northern Highlands Terrane: evidence for lower-crust/upper-mantle relationships. Contrib Mineral Petrol 142:178–197
Vander Auwera J, Bologne G, Roelandts I, Duchesne J-C (1998) Inductively coupled plasma-mass spectrometric (ICP-MS) analysis of silicate rocks and minerals. Geol Belg 1:49–53
Vidal P, Dupuy C, Maury R, Richard M (1989) Mantle metasomatism above subduction zones: Trace-element and radiogenic isotope characteristics of peridotites xenoliths from Batan Island (Philippines). Geology 17:1115–1118
Villaseca C, Downes H, Pin C, Barbero L (1999) Nature and composition of the lower continental crust in central Spain and the granulite-granite linkage: Inferences from granulitic xenoliths. J Petrol 40:1465–1496
Villiger S, Ulmer P, Müntener O, Thompson AB (2004) The liquid line of descent of anhydrous mantle-derived tholeiitic liquids by fractional and equilibrium crystallisation: An experimental study at 1.0 GPa. J Petrol 45:2369–2388
Zeyen H., Novak O, Landes M, Prodehl C, Driad L, Hirn A (1997) Refraction-seismic investigations of the northern massif Central (France). Tectonophysics 275:99–117